
Ground state energy of noninteracting fermions with a random energy spectrum

HENDRIK SCHAWÉ¹, ALEXANDER K. HARTMANN¹, SATYA N. MAJUMDAR² and GRÉGORÉ SCHEHR²

¹ *Institut für Physik, Universität Oldenburg, 26111 Oldenburg, Germany*

² *Univ. Paris-Sud, CNRS, LPTMS, UMR 8626, Orsay F-91405, France*

PACS 05.10.Ln – Monte Carlo methods
PACS 75.10.Nr – Spin-glass and other random models
PACS 05.20.-y – Classical statistical mechanics

Abstract –We derive analytically the full distribution of the ground-state energy of K non-interacting fermions in a disordered environment, modelled by a Hamiltonian whose spectrum consists of N i.i.d. random energy levels with distribution $p(\varepsilon)$ (with $\varepsilon \geq 0$), in the same spirit as the “Random Energy Model”. We show that for each fixed K , the distribution $P_{K,N}(E_0)$ of the ground-state energy E_0 has a universal scaling form in the limit of large N . We compute this universal scaling function and show that it depends only on K and the exponent α characterizing the small ε behaviour of $p(\varepsilon) \sim \varepsilon^\alpha$. We compared the analytical predictions with results from numerical simulations. For this purpose we employed a sophisticated importance-sampling algorithm that allowed us to obtain the distributions over a large range of the support down to probabilities as small as 10^{-160} . We found asymptotically a very good agreement between analytical predictions and numerical results.

The celebrated “Random Energy Model” (REM) of Derrida [1] has continued to play a central role in understanding different aspects of classical disordered systems, including spin-glasses, directed polymers in random media and many other systems. In the REM, one typically has N energy levels which are considered to be independent and identically distributed (i.i.d.) random variables, each drawn from a probability distribution function (PDF) $p(\varepsilon)$. Typical observables of interest are the partition function, free energy, etc. The REM can also be useful as a toy model in quantum disordered systems. For example, let us consider a single quantum particle in a disordered medium with the Hamiltonian \hat{h} . We will assume that the spectrum of the operator \hat{h} has a finite number of states N (for instance a quantum particle on a lattice of finite size and a random onsite potential, as in the Anderson model). In general, solving exactly the spectrum of such an operator is hard, for a generic random potential. One possible approximation, in the spirit of the REM in classical disordered systems, would be to consider the toy model where one replaces the spectrum of the actual Hamiltonian by N ordered i.i.d. energy levels $\varepsilon_1 \leq \varepsilon_2 \leq \dots \leq \varepsilon_N$ each drawn from the common PDF $p(\varepsilon)$. Without loss of generality, we will also assume that the Hamiltonian \hat{h} has only positive eigenvalues. This would mean that, in the corresponding toy model, the PDF $p(\varepsilon)$ is supported on $[0, +\infty)$. It is well known that, in a strongly disordered quantum system, where all single-particle eigenfunctions are localised in space, the energy levels can be approximated by i.i.d. random variables (see *e.g.* [2]). Therefore the

39 REM that we consider here will be relevant in such strongly localised part of the spectrum
40 of a disordered Hamiltonian.

41 Now consider a system of K noninteracting fermions with the Hamiltonian $\hat{H}_K =$
42 $\sum_{i=1}^K \hat{h}_i$ where \hat{h}_i is the single particle Hamiltonian associated with the i -th particle. The
43 ground state of this many-body system would correspond to filling up the single particle
44 spectrum up to the Fermi level ε_K , with one particle occupying each of the states with
45 energies $\varepsilon_1, \varepsilon_2, \dots, \varepsilon_K$. The ground state energy E_0 of this many-body system is therefore
46 given by

$$E_0 = \sum_{i=1}^K \varepsilon_i . \quad (1)$$

47 Clearly, E_0 is a random variable, which fluctuates from one realisation of the disorder to
48 another. Given $p(\varepsilon)$, we are interested in computing the distribution $P_{K,N}$ of E_0 , for fixed
49 K (*i.e.* the number of fermions) and N (*i.e.* the number of levels). We note that, for $K = 1$,
50 $E_0 = \varepsilon_1$ is just the minimum of a set of N i.i.d. random variables and is described by
51 the well-known extreme value statistics [3]. Thus, for general value of K , in particular, it
52 would be interesting to know how sensitive the distribution of E_0 is to the choice of $p(\varepsilon)$.
53 For instance, is there any universal feature of the distribution of E_0 that is independent of
54 $p(\varepsilon)$? We note that E_0 is a sum of random variables, but these random variables are not
55 independent due to the ordering $\varepsilon_1 \leq \varepsilon_2 \leq \dots \leq \varepsilon_N$ (even though the original unordered
56 random variables are independent). Had they been independent, the sum E_0 in eq. (1),
57 by virtue of the Central Limit Theorem, would converge to a shifted and scaled Gaussian
58 random variable. Here, this is not the case, as the ordering induces non-trivial correlations
59 between these variables.

60 In this paper, we compute exactly the PDF $P_{K,N}(E_0)$ for arbitrary K , N and $p(\varepsilon)$ and
61 show that, indeed, a universal feature emerges in the large N limit. It turns out that the
62 limiting distribution of E_0 , for large N , depends only on the small ε behaviour of $p(\varepsilon) \approx B \varepsilon^\alpha$,
63 with $\alpha > -1$, but is otherwise independent of the rest of the features of $p(\varepsilon)$. For fixed α
64 and fixed K , as $N \rightarrow \infty$, we show that the distribution of the ground state energy converges
65 to a limiting scaling form

$$P_{K,N}(E_0) \approx b N^{\frac{1}{\alpha+1}} F_K^{(\alpha)} \left(b N^{\frac{1}{\alpha+1}} E_0 \right) \quad (2)$$

66 where $b = (B/(\alpha + 1))^{1/(\alpha+1)}$ is just a scale factor. The scaling function $F_K^{(\alpha)}(z)$ (with
67 $z \in [0, +\infty)$) is universal and depends only on α and K . We show that the Laplace transform
68 of $F_K^{(\alpha)}(z)$ is given explicitly by

$$\int_0^\infty F_K^{(\alpha)}(z) e^{-\lambda z} dz = \frac{(\alpha + 1)^K}{\Gamma(K) \lambda^{(\alpha+1)(K-1)}} \int_0^\infty x^\alpha e^{-\lambda x - x^{\alpha+1}} [\gamma(\alpha + 1, \lambda x)]^{K-1} dx , \quad (3)$$

69 where $\gamma(a, x) = \int_0^x du u^{a-1} e^{-u}$ is the incomplete gamma function. While we can invert
70 formally this Laplace transform (3), it does not have a simple expression for generic α .
71 However, we can derive the asymptotic behaviour of $F_K^{(\alpha)}(z)$

$$F_K^{(\alpha)}(z) \approx \begin{cases} c_1 z^{(\alpha+1)K-1} , & z \rightarrow 0 , \\ c_2 z^\alpha \exp \left[- \left(\frac{z}{K} \right)^{\alpha+1} \right] , & z \rightarrow \infty , \end{cases} \quad (4)$$

72 where $c_1 = \frac{[\Gamma(\alpha+2)]^K}{\Gamma(K+1)\Gamma((\alpha+1)K)}$ and $c_2 = \frac{(\alpha+1)K^{K-\alpha-2}}{\Gamma(K)}$ are constants. For the extreme-value
73 case $K = 1$ our result, $F_1^{(\alpha)}(z) = (\alpha + 1) z^\alpha e^{-z^{\alpha+1}}$, coincides with the well known Weibull

scaling function [3]. Note that here we are interested in the sum of K lowest i.i.d. variables supported over $[0, +\infty)$. We remark that in the statistics literature, in a completely different context, the sum of the top K values of a set of i.i.d. random variables with an unbounded support has been studied [4, 5]. However, we have not found our results (2) and (3) in the statistics literature.

We start with a set of N positive i.i.d. random variables $\{x_1, x_2, \dots, x_N\}$, each drawn from a common distribution $p(x)$, supported on $[0, +\infty)$. The joint distribution of these variables is simply $P(x_1, \dots, x_N) = \prod_{i=1}^N p(x_i)$. At this stage, these variables are unordered. We are interested in the first K ordered variables $\{\varepsilon_1, \varepsilon_2, \dots, \varepsilon_K\}$ with $K \leq N$. This ordering makes these K variables correlated. Indeed, the joint distribution of the K lowest ordered variables can be written explicitly as

$$P(\varepsilon_1, \dots, \varepsilon_K) = \frac{\Gamma(N+1)}{\Gamma(N-K+1)} \prod_{i=1}^K p(\varepsilon_i) \prod_{i=2}^K \Theta(\varepsilon_i - \varepsilon_{i-1}) \left[\int_{\varepsilon_K}^{\infty} p(u) du \right]^{N-K}. \quad (5)$$

This result can be easily understood as follows. We first choose the K distinct variables from an i.i.d. set of N variables. The number of ways this can be done is simply the combinatorial factor $N(N-1)\dots(N-K+1) = \Gamma(N+1)/\Gamma(N-K+1)$ in eq. (5). The probability that they are ordered is $\prod_{i=1}^K p(\varepsilon_i) \prod_{i=2}^K \Theta(\varepsilon_i - \varepsilon_{i-1})$, where the Heaviside theta functions ensure the ordering. In addition, we have to ensure that the $N-K$ remaining variables are bigger than ε_K , *i.e.* the largest value among the first K ordered variables. Since these $N-K$ variables are i.i.d., this gives the last factor in eq. (5). The formula in eq. (5) is exact for any $p(\varepsilon)$, K and N . Given the joint PDF (5), we are interested in the distribution $P_{K,N}(E_0)$ of the ground-state energy E_0 in eq. (1). We therefore have

$$P_{K,N}(E_0) = \int P(\varepsilon_1, \dots, \varepsilon_K) \delta\left(E_0 - \sum_{i=1}^K \varepsilon_i\right) \prod_{i=1}^K d\varepsilon_i. \quad (6)$$

The form of this equation naturally suggests to consider the Laplace transform with respect to (w.r.t.) E_0

$$\langle e^{-sE_0} \rangle = \int_0^{\infty} P_{K,N}(E_0) e^{-sE_0} dE_0. \quad (7)$$

Taking the Laplace transform of eq. (6) gives

$$\langle e^{-sE_0} \rangle = \frac{\Gamma(N+1)}{\Gamma(N-K+1)} \int_0^{\infty} d\varepsilon_K p(\varepsilon_K) e^{-s\varepsilon_K} \left[\int_{\varepsilon_K}^{\infty} p(u) du \right]^{N-K} J_{K-1}(\varepsilon_K), \quad (8)$$

where

$$J_{K-1}(\varepsilon_K) = \int \prod_{i=1}^{K-1} p(\varepsilon_i) e^{-s\varepsilon_i} d\varepsilon_i \prod_{i=2}^K \Theta(\varepsilon_i - \varepsilon_{i-1}). \quad (9)$$

This multiple integral (9) has a nested structure and can be evaluated easily by induction and one gets

$$J_{K-1}(\varepsilon_K) = \frac{1}{(K-1)!} \left[\int_0^{\varepsilon_K} du e^{-su} p(u) \right]^{K-1}. \quad (10)$$

Using this result in eq. (8), and also replacing, for later convenience, $\int_y^{\infty} du p(u) = 1 - \int_0^y du p(u)$, we get the exact formula

$$\langle e^{-sE_0} \rangle = K \binom{N}{K} \int_0^{\infty} dy p(y) e^{-sy} \left[1 - \int_0^y du p(u) \right]^{N-K} \left[\int_0^y dv p(v) e^{-sv} \right]^{K-1}. \quad (11)$$

102 This formula has a simple interpretation. Taking the Laplace transform is equivalent to
103 breaking the system into two species of random variables of size K and $N - K$ (this can be
104 done in $\binom{N}{K}$ ways): Each member of the first species of size K comes with an effective weight
105 $p(\varepsilon) e^{-s\varepsilon}$, while in the second species of size $N - K$ each member comes with an effective
106 weight $p(\varepsilon)$. We first fix the K -th variable to have a value y , whose weight is $p(y) e^{-sy}$.
107 The members of the second species should each be bigger than y (explaining the factor
108 $\left[\int_y^\infty p(u) du \right]^{N-K}$), while the rest of the $(K - 1)$ members of the first species should each
109 be smaller than y , explaining the factor $\left[\int_0^y dv e^{-sv} p(v) \right]^{K-1}$. Finally, the biggest variable
110 among the members of the first species can be any of the K members, explaining the factor
111 K multiplying the binomial coefficient $\binom{N}{K}$ in eq. (11). With this interpretation, it is clear
112 that eq. (11) can be easily generalized to any linear statistics of the form $L_K = \sum_{i=1}^K f(\varepsilon_i)$
113 where $f(\varepsilon)$ is an arbitrary function. The ground state energy E_0 considered here corresponds
114 to choosing $f(\varepsilon) = \varepsilon$. For general $f(\varepsilon)$ the effective weight of each member of the first species
115 discussed above is just $p(\varepsilon) e^{-sf(\varepsilon)}$. Hence the formula in eq. (11) generalises to

$$\langle e^{-sL_K} \rangle = K \binom{N}{K} \int_0^\infty dy p(y) e^{-sf(y)} \left[\int_y^\infty p(u) du \right]^{N-K} \left[\int_0^y dv p(v) e^{-sf(v)} \right]^{K-1}. \quad (12)$$

116 In this paper, we will focus only on the case $f(\varepsilon) = \varepsilon$. Below, we thus start with the exact
117 result in eq. (11) and analyse its behaviour in the large N limit.

118 To understand the large N scaling limit, it is instructive to start with the $K = 1$ case.
119 In this case, $E_0 = \varepsilon_1$ is just the minimum of a set of N i.i.d. random variables, each drawn
120 from $p(\varepsilon)$. In this case, eq. (11) reads (upon setting $K = 1$)

$$\langle e^{-sE_0} \rangle = N \int_0^\infty dy p(y) e^{-sy} \left[1 - \int_0^y du p(u) \right]^{N-1}, \quad (13)$$

121 where we replaced $\int_y^\infty du p(u) = 1 - \int_0^y du p(u)$, using the normalisation of $p(u)$. In the
122 large N limit, the dominant contribution to the integral over y comes from the regime of y
123 where the integral $\int_0^y du p(u)$ is of order $O(1/N)$. For other values of y , the contribution is
124 exponentially small in N , for large N . Hence, we see that, in the large N limit, only the
125 small y behaviour of $p(y)$ matters. Let

$$p(y) \underset{y \rightarrow 0}{\approx} B y^\alpha \quad (14)$$

126 where $\alpha > -1$ in order that $p(y)$ is normalisable and clearly $B > 0$. Substituting this leading
127 order behaviour of $p(y)$ for small y (14) in eq. (13), we get

$$\langle e^{-sE_0} \rangle \approx B N \int_0^\infty dy y^\alpha e^{-sy} \exp\left(-\frac{BN}{\alpha+1} y^{\alpha+1}\right). \quad (15)$$

128 Performing the change of variable $y = \left(\frac{\alpha+1}{BN}\right)^{\frac{1}{\alpha+1}} x$, we get

$$\langle e^{-sE_0} \rangle \approx (\alpha+1) \int_0^\infty dx x^\alpha \exp\left(-\frac{s}{b N^{\frac{1}{\alpha+1}}} x - x^{\alpha+1}\right), \quad (16)$$

129 where $b = (B/(\alpha+1))^{1/(\alpha+1)}$. Inverting the Laplace transform formally, we obtain the
130 scaling form given in eq. (2) with $K = 1$ and the scaling function $F_1^{(\alpha)}(z)$ has its Laplace
131 transform as in (3) with $K = 1$. Inverting this Laplace transform exactly, we recover the
132 Weibull scaling function $F_1^{(\alpha)}(z) = (\alpha+1)z^\alpha e^{-z^{\alpha+1}}$. The calculation for $K = 1$ shows that
133 only the small y behaviour of $p(y)$ matters in the limit of large N . Furthermore, for $K = 1$,
134 we see that the typical value of E_0 scales as $N^{-\frac{1}{\alpha+1}}$ for large N . We then anticipate that,

even for $K > 1$, the typical scale of E_0 will remain the same $E_0 \sim N^{-\frac{1}{\alpha+1}}$ for large N . Below, we indeed use this typical scale for E_0 (and verify a posteriori) and compute the scaling function $F_K^{(\alpha)}(z)$ for general K in eq. (2).

We now derive the main results in Eqs. (2) and (3) for all $K \geq 1$. Anticipating the scaling $E_0 \sim N^{-\frac{1}{\alpha+1}}$ as mentioned above, we set

$$E_0 = \frac{1}{b} N^{-\frac{1}{\alpha+1}} z, \quad (17)$$

where b is a constant to be fixed later and the scaled ground state energy z is of order $O(1)$. Substituting this scaling form (17) in eq. (11), we see that the left hand side (l.h.s.) reads, $\langle e^{-sE_0} \rangle = \langle e^{-sN^{-\frac{1}{\alpha+1}} z/b} \rangle = \langle e^{-\lambda z} \rangle$ where $\lambda = N^{-\frac{1}{\alpha+1}} s/b$ is the rescaled Laplace variable. We will take the $N \rightarrow \infty$ limit, keeping λ fixed. This then corresponds to $s \rightarrow \infty$ limit. On the right hand side (r.h.s.) of eq. (11) we make a change of variable $sy = \tilde{x}$ as well as $u = \tilde{u}/s$ and $v = \tilde{v}/s$. This gives

$$\langle e^{-\lambda z} \rangle = \frac{K}{s^K} \binom{N}{K} \int_0^\infty d\tilde{x} p\left(\frac{\tilde{x}}{s}\right) e^{-\tilde{x}} \left(1 - \frac{1}{s} \int_0^{\tilde{x}} d\tilde{u} p\left(\frac{\tilde{u}}{s}\right)\right)^{N-K} \left(\int_0^{\tilde{x}} d\tilde{v} p\left(\frac{\tilde{v}}{s}\right) e^{-\tilde{v}}\right)^{K-1}. \quad (18)$$

In the large s limit, we use $p(y) \approx By^\alpha$ to leading order. Inserting this behaviour in eq. (18), we get

$$\langle e^{-\lambda z} \rangle \approx \frac{K B^K}{s^{(\alpha+1)K}} \binom{N}{K} \int_0^\infty d\tilde{x} \tilde{x}^\alpha e^{-\tilde{x}} \left(e^{-\frac{B(N-K)}{(\alpha+1)s^{\alpha+1}} \tilde{x}^{\alpha+1}}\right) [\gamma(\alpha, \tilde{x})]^{K-1} \quad (19)$$

where we recall that $\gamma(a, x) = \int_0^x du u^{a-1} e^{-u}$ is the incomplete gamma function. We now use $s = (\lambda b) N^{\frac{1}{\alpha+1}}$ and choose

$$b = \left(\frac{B}{\alpha+1}\right)^{\frac{1}{\alpha+1}}. \quad (20)$$

Furthermore, in the large N limit $\binom{N}{K} \sim N^K/\Gamma(K)$. Using these results, and rescaling $\tilde{x} = \lambda x$, we arrive at

$$\langle e^{-\lambda z} \rangle = \frac{(\alpha+1)^K}{\Gamma(K)\lambda^{(\alpha+1)(K-1)}} \int_0^\infty dx x^\alpha e^{-\lambda x - x^{\alpha+1}} [\gamma(\alpha+1, \lambda x)]^{K-1} dx. \quad (21)$$

This clearly shows that the distribution of the rescaled random variable $z = (E_0 b) N^{\frac{1}{\alpha+1}}$ [see eq. (17)] converges to an N -independent form $F_K^{(\alpha)}(z)$ for large N , whose Laplace transform is given by $\int_0^\infty F_K^{(\alpha)}(z) e^{-\lambda z} dz = \langle e^{-\lambda z} \rangle$. Therefore eq. (21) demonstrates the result announced in eq. (3).

Special cases $\alpha = 0$. In this case eq. (3), using $\gamma(1, \lambda x) = 1 - e^{-\lambda x}$, reduces to

$$\int_0^\infty F_K^{(0)}(z) e^{-\lambda z} dz = \frac{1}{\Gamma(K)\lambda^{K-1}} \int_0^\infty dx e^{-(\lambda+1)x} (1 - e^{-\lambda x})^{K-1} = \frac{\Gamma(1+1/\lambda)}{\lambda^k \Gamma(k+1+1/\lambda)}. \quad (22)$$

Using the properties of the Γ function, one can express the r.h.s. of (22) as a simple product

$$\int_0^\infty F_K^{(0)}(z) e^{-\lambda z} dz = \prod_{m=1}^K \frac{1}{1+m\lambda}. \quad (23)$$

152 To invert this Laplace transform, we note that the r.h.s. has simple poles at $\lambda = -1/m$ with
 153 $m = 0, 1, \dots, K$. Evaluating carefully the residues at these poles, we can invert this Laplace
 154 transform explicitly and get

$$F_K^{(0)}(z) = \sum_{n=1}^K (-1)^{K-n} \frac{n^{K-1}}{(K-n)! n!} e^{-z/n}. \quad (24)$$

155 For instance,

$$F_1^{(0)}(z) = e^{-z} \quad (25)$$

$$F_2^{(0)}(z) = e^{-z/2} - e^{-z} \quad (26)$$

$$F_3^{(0)}(z) = \frac{3}{2} e^{-z/3} - 2 e^{-z/2} + \frac{1}{2} e^{-z}. \quad (27)$$

156 *Numerical simulations.* Next, we verify our analytical predictions via numerical simulations.
 157 To test the prediction of the scaling behaviour in eq. (2), as well as to test the universality of
 158 the associated scaling function $F_K^{(\alpha)}(z)$, we consider four different distributions for the energy
 159 levels: (a) an exponential distribution $p(\varepsilon) = e^{-\varepsilon} \Theta(\varepsilon)$, (b) an half-Gaussian distribution
 160 $p(\varepsilon) = \sqrt{\frac{2}{\pi}} e^{-\varepsilon^2} \Theta(\varepsilon)$, (c) a Pareto distribution $p(\varepsilon) = \frac{2}{\varepsilon^3} \Theta(\varepsilon - 1)$ and (d) $p(\varepsilon) = \varepsilon e^{-\varepsilon} \Theta(\varepsilon)$.
 161 The cases (a) and (b) clearly correspond to $\alpha = 0$. Hence we expect the scaling function
 162 to be given by $F_K^{(0)}(z)$ in eq. (24). The Pareto case (c), with support over $[1, +\infty)$, also
 163 corresponds to the $\alpha = 0$ case, as seen easily after a trivial shift $\varepsilon \rightarrow \varepsilon - 1$. Hence, in
 164 this case as well, we expect the scaling function to be given by $F_K^{(0)}(z)$. However, case (d)
 165 is different as it corresponds to $\alpha = 1$ and hence the scaling function should be given by
 166 $F_K^{(1)}(z)$. In fig. 1, we compare the simulation results with the analytical predictions and find
 167 very good agreement. Note that in cases (a)-(c), the scaling function $F_K^{(0)}(z)$ has an explicit
 168 expression as in eq. (24). Hence, it is easy to compare directly the simulation results with
 169 this expression (as in fig. 1 (a)-(c)). However, for case (d), where $\alpha = 1$, we do not have a
 170 simple explicit formula for $F_K^{(1)}(z)$, though we have explicitly given its Laplace transform in
 171 eq. (3) with $\alpha = 1$. Hence, to compare with the simulation results, we first needed to invert
 172 this Laplace transform using an arbitrary precision library [21]. This comparison is shown
 173 in fig. 1 (d).

174 To obtain the presented numerical results one has to generate N random numbers ac-
 175 cording to the desired probability density $p(\varepsilon)$. This is done by a standard method, namely
 176 we first choose a uniform random number $\eta \in [0, 1]$ and then generate ε using the formula,
 177 $\int_0^\varepsilon p(\varepsilon') d\varepsilon' = \eta$. The exponential (a) and Pareto (c) case can be trivially obtained using this
 178 relation [6]. In the half-Gaussian case (b), the Gaussian random numbers can be generated
 179 using the Box-Muller method [6]. In the case (d), $p(\varepsilon) = \varepsilon e^{-\varepsilon}$, the above relation reads
 180 $\eta = \int_0^\varepsilon p(\varepsilon') d\varepsilon' = 1 - (1 + \varepsilon) e^{-\varepsilon}$, which can also be inverted using the -1 branch of the
 181 Lambert W function [8] $\varepsilon = -W_{-1} \left(\frac{\eta-1}{e} \right) - 1$. To evaluate the Lambert W function, we use
 182 the GSL implementation [7].

183 The sum E_0 in eq. (1) is completely determined by the values $\boldsymbol{\eta} = (\eta_1, \dots, \eta_N)$. If
 184 one simply generates many times vectors $\boldsymbol{\eta}$ of independent uniform random numbers and
 185 correspondingly obtained random numbers $(\varepsilon_1, \dots, \varepsilon_N)$, one will obtain only typical results
 186 for E_0 , *i.e.* those having a high enough probability. Here, we sample the distributions over
 187 a broad range of the support, also in the far tails, where the probabilities are extremely
 188 small. For this purpose, we use a well tested importance sampling scheme [9, 10]. Here
 189 the vectors $\boldsymbol{\eta}$ are sampled using the Metropolis algorithm including a bias of samples away
 190 from the main part of the distribution. We use a bias $e^{-E_0/T}$, where T is a ‘‘temperature’’
 191 parameter which can be positive and negative and allows us to address different ranges of
 192 the distribution. Since the bias is known, the Metropolis results can be corrected for the

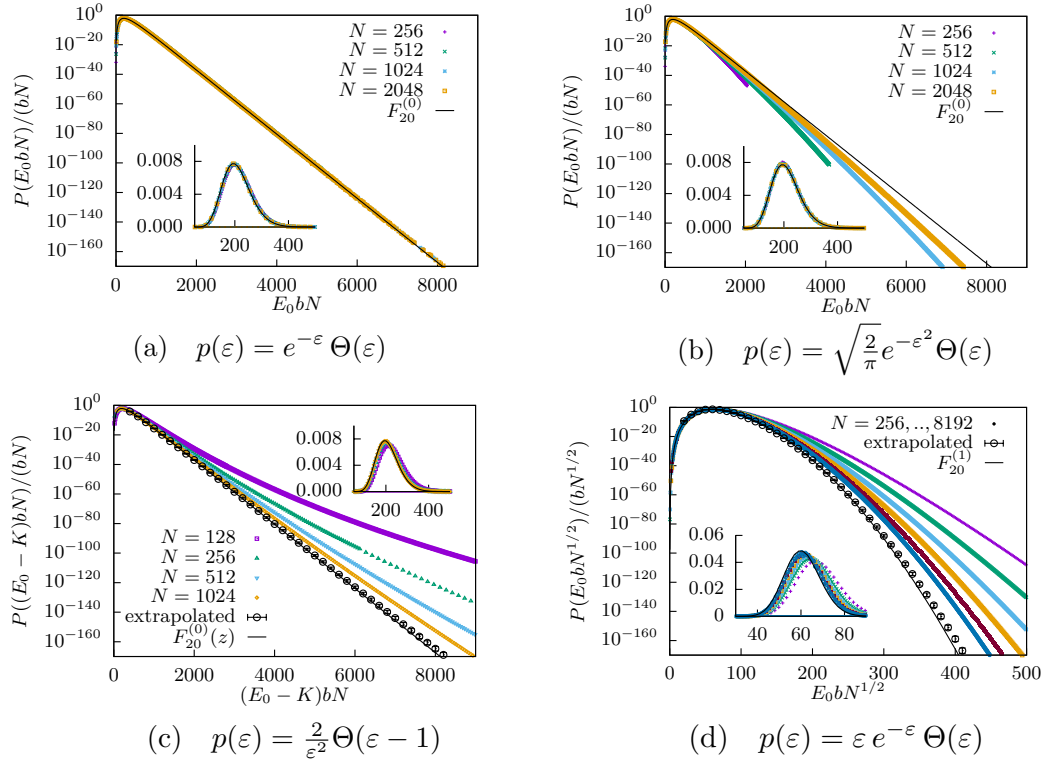


Fig. 1: (colour online) Scaled distribution $P_{K,N}(E_0)$ for $K = 20$, for different values of N and for four different distribution $p(\varepsilon)$. The insets show the behaviour near the peaks for the four different cases. (a) shows exponentially distributed $p(\varepsilon) = e^{-\varepsilon} \Theta(\varepsilon)$ which corresponds to $\alpha = 0$ and $b = 1$ [see eq. (2)]. The scaling function $F_{K=20}^{(0)}$ in eq. (24) matches very well the numerical data all the way up to the tails. (b) shows half-Gaussian distributed $p(\varepsilon) = \frac{\sqrt{2}}{\sqrt{\pi}} e^{-\varepsilon^2/2} \Theta(\varepsilon)$ corresponding to $\alpha = 0$ and $b = p(0) = \frac{2}{\sqrt{2\pi}}$. (c) shows Pareto distributed energy levels $p(\varepsilon) = \frac{2}{\varepsilon^2} \Theta(\varepsilon - 1)$. After shifting $\varepsilon \rightarrow \varepsilon - 1$, *i.e.* $E_0 \rightarrow E_0 - K$, this falls in the $\alpha = 0$ universality, with $b = 2$. In this case, using the finite-size extrapolation scheme shown in black circles (see text and eq. (30) with $\beta = 1$), the data approach the theoretical scaling function $F_{20}^{(0)}(z)$. (d) shows energy levels distributed according to $p(\varepsilon) = \varepsilon e^{-\varepsilon} \Theta(\varepsilon)$. This corresponds to the $\alpha = 1$ universality class, with the scaling parameter $b = 1/\sqrt{2}$. Again, using the finite-size scaling form (see text and eq. (30)) with $\beta = 1/2$, the extrapolated data (shown in black circles) match well with the theoretical scaling function $F_{20}^{(1)}(z)$, obtained from the numerical Laplace inversion of eq. (3), setting $K = 20$ and $\alpha = 1$.

193 bias to obtain the actual distribution. This enables us to gather good statistics also in the
 194 far tails.

To be more concrete, we use a Markov chain $\boldsymbol{\eta}(t) = \boldsymbol{\eta}(0), \boldsymbol{\eta}(1), \dots$. Every move $\boldsymbol{\eta}(t) \rightarrow \boldsymbol{\eta}(t+1)$ consists of changing one entry of $\boldsymbol{\eta}(t)$ leading to a trial $\boldsymbol{\eta}'$ (“local update”). While the most simple method to change would be the replacement of one uniform-distributed random number by a freshly drawn one, as used in Ref. [10], this will lead to difficulties especially for small values K . For the far tails, there will be a point where all entries of $\boldsymbol{\eta}$ are almost one (or almost zero) and almost every new proposal will be rejected, since it is improbable to draw a random number very close to the previous one. Therefore we perform a slightly more involved protocol, where instead of redrawing we change an entry $\eta_i \rightarrow \eta_i + \xi \delta$, where $\xi \in [-1, 1]$ is uniformly distributed and $\delta \in \{10^{-i} | i \in \{0, 1, 2, 3, 4, 5\}\}$ with uniform probability $1/6$. Thus δ determines the scale of the local change. Changes resulting in an entry $\eta_i \notin [0, 1)$ are directly *rejected*, *i.e.* $\boldsymbol{\eta}(t+1) = \boldsymbol{\eta}(t)$. Note that this

protocol will still result in uniformly distributed random numbers η_i , if every change in $[0, 1)$ was *accepted*, *i.e.* $\boldsymbol{\eta}(t + 1) = \boldsymbol{\eta}'$. Here each proposed change is accepted instead with the Metropolis acceptance ratio

$$p_{\text{acc}} = \min\{1, e^{-\Delta E_0/T}\}, \quad (28)$$

195 where ΔE_0 is the change in energy caused by the proposed change, and otherwise also
196 rejected.

For any value of T , as usual for Monte Carlo simulations, performing these Markov chains “long enough” and taking measurements, this results in a histogram $P_T(E_0)$ for each temperature, which can be corrected for the bias using

$$P(E_0) = e^{E_0/T} Z(T) P_T(E_0). \quad (29)$$

197 The a-priori unknown normalization parameter $Z(T)$ can be obtained by enforcing continuity
198 and normalization of the whole distribution, which is obtained from performing simulations
199 for several values of T , including $T = \infty$, which corresponds to simple sampling. We will not
200 go into further details, since this algorithm is well described in several other publications
201 [9–11].

202 For the Pareto distributed case $p(\varepsilon) = \frac{2}{\varepsilon^3} \Theta(\varepsilon - 1)$, we used instead of the aforemen-
203 tioned sampling with bias $e^{E_0/T}$ a modified *Wang-Landau* sampling [12–16] with multiple
204 histograms and subsequent entropic sampling [17, 18]. We used Wang Landau sampling for
205 this case, since the temperatures are harder to adjust, *i.e.* for negative temperatures it hap-
206 pens quickly that equilibration becomes impossible and the energy increases constantly. This
207 effect is already known to pose difficulties for the aforementioned sampling with bias [19, 20].

208 We set $K = 20$ in fig. 1 and compare the distribution $P_{K=20,N}(E_0)$ for different values
209 of N . We verify, by a data collapse, the scaling form predicted in eq. (2) and also compare
210 the numerical scaling function to the analytical ones. As mentioned earlier, for the $\alpha = 0$
211 case (corresponding to cases (a)-(c)), the analytical scaling function is given in eq. (24). For
212 the $\alpha = 1$ (corresponding to case (d)), we invert the Laplace transform in eq. (3) for $K = 20$
213 and $\alpha = 1$, using an arbitrary precision library [21].

214 While the exponential case fits very well to the analytic result even for small values of
215 N , the other cases show strong finite-size effects especially in the extreme right tail. Such
216 finite-size effects are known to occur frequently in the extreme statistics of i.i.d. random
217 variables [22]. As seen in fig. 1, the discrepancy between the numerical and the analytical
218 results is very small in the main region (*i.e.* in the bulk). In the tails, we need to use a
219 finite-size ansatz to study the convergence of the numerical results as $N \rightarrow \infty$. For example,
220 it is natural to expect that the finite-size corrections to the leading scaling form in eq. (2)
221 is of the form

$$P_{K,N}(E_0) = b N^{1/(1+\alpha)} \left[F_K^{(\alpha)}(z) + N^{-\beta} G_K^{(\alpha)}(z) + N^{-2\beta} H_K^{(\alpha)}(z) + \dots \right], \quad (30)$$

222 where $\beta = \min(1/(1 + \alpha), 1)$, $z = b N^{1/(\alpha+1)} E_0$ is the scaling variable, and $G_K^{(\alpha)}(z), H_K^{(\alpha)}(z)$
223 describe the finite-size scaling of the correction terms. Thus for $\alpha = 0$ one has $\beta = 1$,
224 while for $\alpha = 1$, we have $\beta = 1/2$. For several values of z , we extrapolate the data by
225 fitting pointwise the numerical data in fig. 1 as a function of N , to obtain estimates for the
226 asymptotes $F_K^{(\alpha)}(z)$. We treated the cases (c) (corresponding to $\alpha = 0$, and hence $\beta = 1$) and
227 (d) ($\alpha = 1, \beta = 1/2$), the extrapolated values are shown as symbols. Furthermore, in fig. 2,
228 we show the behaviour in the tails for the case (d), which exhibits the strongest finize-size
229 effects, such that the asymptotic behaviour eq. (4) is directly visible. It is apparent that the
230 convergence for large values of N is faster in the left tail $z \rightarrow 0$, while it is much slower in
231 the right tail $z \rightarrow \infty$.

232 *Conclusion.* In this paper, we have studied analytically and numerically the full distribu-
233 tion of the ground-state energy of K non-interacting fermions in a disordered environment,

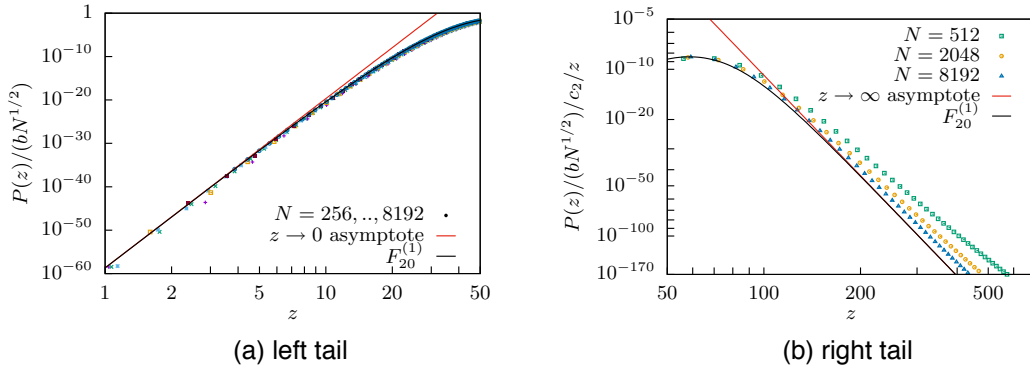


Fig. 2: (colour online) We consider the tails of the distribution $P_{K=20,N}(E_0)$ for the case $p(\varepsilon) = \varepsilon e^{-\varepsilon}$, corresponding to $\alpha = 1$. This scaling function in this case is given by $F_{K=20}^{(1)}(z)$. The asymptotic behaviors of $F_{K=20}^{(1)}(z)$ in eq. (4), for $z \rightarrow 0$ (left tail, in (a)) and $z \rightarrow \infty$ (right tail in (b)) are compared to numerical simulations. The data have been plotted on a scale such that the two cases from eq. (4) appear as straight lines. In (b), for clarity, only three different values of N have been plotted.

modelled by a Hamiltonian whose spectrum consists of N i.i.d. random energy levels with distribution $p(\varepsilon)$ (with $\varepsilon \geq 0$), in the same spirit as the “Random Energy Model”. This ground state energy is the sum of the smallest K values drawn from a probability distribution and therefore a generalization of the extrem-value statistics, which corresponds to the case $K = 1$. Thus our results should be of interest also in a very general mathematical context.

We have shown that for each fixed K , the distribution $P_{K,N}(E_0)$ of the ground-state energy has a universal scaling form in the limit of large N (see eq. (2)). This universal distribution depends only on K and the exponent α characterizing the small ε behaviour of $p(\varepsilon) \sim \varepsilon^\alpha$. We derive an exact expression for the Laplace transform of this scaling function in eq. (3). For generic α , the asymptotic behaviors of the scaling function are derived explicitly in eq. (4), while for the special case $\alpha = 0$, the Laplace transform can be explicitly inverted, giving the full scaling function in eq. (24). Numerically, while the peak region of the distribution of E_0 can be easily estimated by standard methods, estimating the tails of the distribution where the probability is very small is hard and requires more sophisticated techniques. In this paper, using an importance sampling algorithm, we were able to estimate the tail probabilities (up to a precision as small as 10^{-160}) and thereby to verify the theoretical predictions. Thus the main conclusion of our work is that, even though the individual energy levels are independent random variables, the ordering needed to compute the ground-state energy induces effective correlations between the energy levels. These effective correlations then lead, for the ground-state energy, to a whole new class of universal scaling functions parameterised by K and α .

In this work, we have modelled the single-particle energy levels of a quantum disordered system by i.i.d. random variables, à la REM. This REM approximation for the energy levels is known to be valid for disordered Hamiltonians whose eigenstates are strongly localised in space [2]. Thus we expect that the results presented in this paper for the universal distribution of the ground state energy would apply to such strongly disordered quantum systems. It is then natural to ask what happens to the ground-state energy for Hamiltonians with weakly localised eigenstates. In some weakly localised systems, a description based on Random Matrix Theory (RMT) [2] is a good approximation, where the energy levels (identified with the eigenvalues of a random matrix) are strongly correlated with mutual level repulsion. In this RMT context, several linear statistics of ordered eigenvalues have been

266 recently introduced and studied for large N under the name of truncated linear statistics
267 (TLS) [23, 24]. The ground-state energy in eq. (1) or more generally the linear statistics
268 as in eq. (12) studied here are instances of TLS, but for i.i.d. random variables. It would
269 thus be interesting to see how the TLS, studied here for i.i.d. variables, crosses over to the
270 RMT case, as one goes from the strongly localised part of the spectrum of a disordered
271 Hamiltonian to the weakly localised part.

* * *

272 This work was supported by the German Science Foundation (DFG) through the grant
273 HA 3169/8-1. HS and AKH thank the LPTMS for hospitality and financial support during
274 one and two-month visits, respectively, where this project was conceived. The simulations
275 were performed at the cluster of the GWDG Göttingen and the HPC cluster CARL, located
276 at the University of Oldenburg (Germany) and funded by the DFG through its Major
277 Research Instrumentation Programme (INST 184/157-1 FUGG) and the Ministry of Science
278 and Culture (MWK) of the Lower Saxony State. SM and GS acknowledge support by ANR
279 grant ANR-17-CE30-0027-01 RaMaTraF.

280 REFERENCES

- 281 [1] B. Derrida, Phys. Rev. B **24**, 2613 (1981).
282 [2] M. Moshe, H. Neuberger, and B. Shapiro, Phys. Rev. Lett. **73**, 1497 (1994).
283 [3] E. J. Gumbel, *Statistics of Extremes*, Dover, New York, (1958).
284 [4] H. N. Nagaraja, Ann. I. Stat. Math. **33**, 437 (1981).
285 [5] H. N. Nagaraja, Ann. Stat. **10**, 1306 (1982).
286 [6] W. H. Press, S. A. Teukolsky, W. T. Vetterling, and B. P. Flannery, Numerical recipes
287 3rd edition: The art of scientific computing (Cambridge university press, 2007), ISBN
288 9780521880688.
289 [7] B. Gough, GNU Scientific Library Reference Manual - Third Edition (Network Theory Ltd.,
290 2009), 3rd ed., ISBN 0954612078, 9780954612078.
291 [8] R. M. Corless, G. H. Gonnet, D. E. G. Hare, D. J. Jeffrey, and D. E. Knuth, Advances in
292 Computational Mathematics **5**, 329 (1996), ISSN 1572-9044.
293 [9] A. K. Hartmann, Phys. Rev. E **65**, 056102 (2002).
294 [10] A. K. Hartmann, Phys. Rev. E **89**, 052103 (2014).
295 [11] H. Schawe, A. K. Hartmann, and S. N. Majumdar, Phys. Rev. E **97**, 062159 (2018).
296 [12] F. Wang and D. P. Landau, Phys. Rev. Lett. **86**, 2050 (2001).
297 [13] F. Wang and D. P. Landau, Phys. Rev. E **64**, 056101 (2001).
298 [14] B. J. Schulz, K. Binder, M. Müller, and D. P. Landau, Phys. Rev. E **67**, 067102 (2003).
299 [15] R. E. Belardinelli and V. D. Pereyra, Phys. Rev. E **75**, 046701 (2007).
300 [16] R. E. Belardinelli and V. D. Pereyra, The Journal of Chemical Physics **127**, 184105 (2007).
301 [17] J. Lee, Phys. Rev. Lett. **71**, 211 (1993).
302 [18] R. Dickman and A. G. Cunha-Netto, Phys. Rev. E **84**, 026701 (2011).
303 [19] G. Claussen, A. K. Hartmann, and S. N. Majumdar, Phys. Rev. E **91**, 052104 (2015).
304 [20] H. Schawe, A. K. Hartmann, and S. N. Majumdar, Phys. Rev. E **96**, 062101 (2017).
305 [21] F. Johansson et al., mpmath: a Python library for arbitrary-precision floating-point arith-
306 metic (version 1.0.0) (2013), <http://mpmath.org/>.
307 [22] G. Gyorgyi, N. R. Moloney, K. Ozogany, Z. Racz, and M. Droz, Phys. Rev. E **81**, 041135
308 (2010).
309 [23] A. Grabsch, S. N. Majumdar, C. Texier, J. Stat. Phys. **167**, 234 (2017).
310 [24] A. Grabsch, S. N. Majumdar, C. Texier, J. Stat. Phys. **167**, 1452 (2017).